

## Modeling of a DR Shaft Operated with Pure Hydrogen Using a Physical-chemical and CFD Approach

A. Ranzani da Costa, D. Wagner, F. Patisson and D. Ablitzer

LSG2M, INPL, CNRS, Nancy-Université, Nancy, France

[fabrice.patisson@mines.inpl-nancy.fr](mailto:fabrice.patisson@mines.inpl-nancy.fr)

The hydrogen-based route could be a valuable way to produce steel considering its low carbon dioxide emissions. In ULCOS, it is regarded as a long-term option, largely dependent on the emergence of a hydrogen economy. To anticipate its possible development, it was decided to check the feasibility of using 100% H<sub>2</sub> in a Direct Reduction shaft furnace and to determine the best operating conditions, through appropriate experimental and modelling work.

We developed from scratch a new model, called REDUCTOR, for simulating this process and predicting its performance. This sophisticated numerical model is based on the mathematical description of the detailed physical, chemical and thermal phenomena occurring. In particular, kinetics were derived from experiments. The current version is suited to the reduction with pure hydrogen, but an extension of the model to CO is planned so that it will also be adapted to the simulation and optimisation of the current DR processes.

First results have confirmed that the reduction with hydrogen is much faster than that with CO, making it possible to design a hydrogen-operated shaft reactor quite smaller than current MIDREX and HYL.

### Introduction

Breakthrough ways for making steel are investigated within the ULCOS (Ultra low CO<sub>2</sub> steelmaking) European program [1], with the target of at least 50 % reduction in CO<sub>2</sub> emissions as compared to these of the current integrated steel plants, i.e. 1844 kg of CO<sub>2</sub>/t of HRC (hot rolled coil). The use of hydrogen as a reducing agent, instead of CO, with an associated production of H<sub>2</sub>O instead of CO<sub>2</sub>, was evaluated in ULCOS SP4 (Hydrogen-based steelmaking) and is further studied in SP12 (Advanced direct reduction), as well as by other groups in the world [2]. The ULCOS SP4's preferred route to steel is shown in Figure 1. Its performance regarding CO<sub>2</sub> emission is promising: down to less than 300 kg CO<sub>2</sub>/t HRC, if hydrogen is produced by water electrolysis using hydraulic or nuclear electricity, without any CO<sub>2</sub> capture necessary [3].

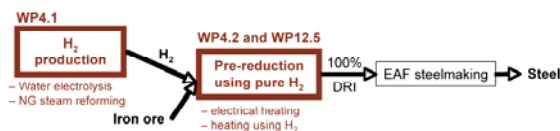


Figure 1. Hydrogen-based route to steel

However, the future development of such a process heavily depends on the emergence of the so-called hydrogen economy, which could result from the demand of other industrial sectors, like energy and transportation industries. It is here assumed that H<sub>2</sub> would become available in this frame, in large quantities, at competitive cost, and with low CO<sub>2</sub> emission for its production. We believe that steelmakers should anticipate and be ready to take profit of such a situation by using hydrogen to a large extent. The present research was performed, at the University of

Nancy, France, to check the feasibility of the reduction of iron ore by pure hydrogen and to define the best processing conditions for the direct reduction in a shaft furnace, through appropriate experimental and modelling work.

### Experiments

Although the reduction of iron ore by hydrogen was extensively studied in the 1970s and 80s (e.g. [4-7]), few publications report kinetic expressions suited to the reduction of industrial pellets and directly usable for modelling. To clarify the mechanisms of the reaction and get accurate kinetic data for reactor modelling, we undertook a series of reduction experiments by thermogravimetry, completed by sample characterization by XRD (X-ray diffraction), SEM (Scanning electron microscopy), and Mössbauer spectrometry.

The thermobalance used was a Setaram Tag24 model, with two symmetrical furnaces, which presents the advantage of eliminating the disruptive effects of buoyancy and drag forces, ensuring  $\mu\text{g}$  accuracy. A specific steam generator was attached to possibly add controlled water content to the reaction gas. Samples were small hematite cubes (5-mm side, 550-mg weight) shaped in CVRD industrial pellets. The reason for making such cubes was the limiting total weight loss imposed by the balance. Reduction experiments were run under isothermal conditions: a single cube was wrapped in a Pt wire and directly hung to the balance beam; when the desired temperature was reached and stabilized, H<sub>2</sub> was introduced into the system and maintained until the end of the reaction. Gas compositions were 100 % H<sub>2</sub> and 60 vol. % H<sub>2</sub> in He. In some cases, up to 4 vol. % H<sub>2</sub>O were added to study the effect of water in the reducing gas. Smaller cubes were also alterna-

tively used. Temperature varied from 600 °C to 990 °C. Its effect (Figure 2) deserves attention and is discussed below.

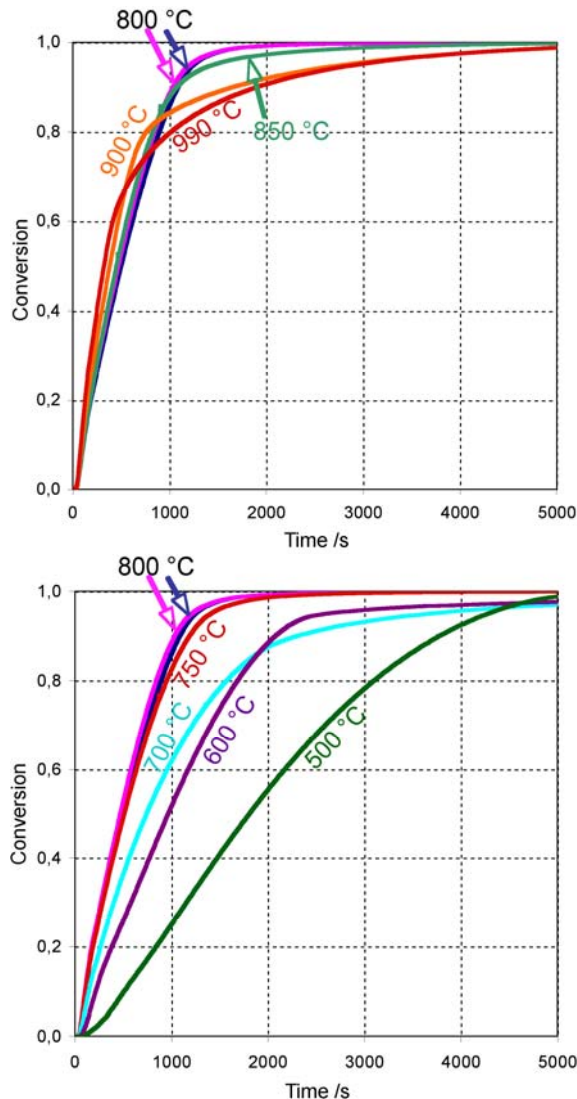


**Figure 2.** Influence of temperature on the reduction curves of hematite cubes, under 60 % H<sub>2</sub> in He

For experiment temperatures up to 800 °C, the higher the temperature, the faster the reaction, except at 700 °C where the reaction is slower. Above 800 °C, an increase in temperature first accelerates the reaction rate, but, when reaching a high conversion, the reaction slows down and goes on at a lower rate, the total reaction time being longer than at 800 °C. Thus, from these experiments, 800 °C appears as an optimum temperature for achieving a full conversion in minimum time.

A series of interrupted experiments, where the hydrogen flow was stopped before complete reduction, were carried out to allow for the characterization of samples at different degrees of conversion. Partly reduced samples were then observed by SEM and analyzed by Mössbauer spectrometry and X-ray diffraction. These experiments helped reveal the course of the reduction, through the formation of intermediate oxides and the corresponding morphological

evolution (Figure 3). The hematite pellet is made up of large, dense grains, separated by thin cracks. The grainy structure only changes slightly from hematite to magnetite and wustite. The main point is the appearance and growth of pores on the sides of the grains. At the stage of wustite, however, cross-sections of grains (bottom right photo) show that these become very porous and sub-divided into smaller grains that we termed “crystallites”. From wustite to iron, the solid structure changes dramatically. Iron forms larger, dense grains. Yet the final inter-grain porosity remains high.

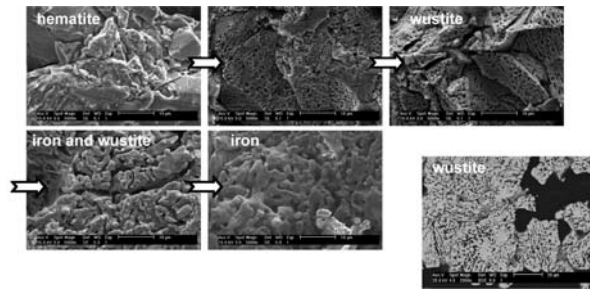


**Figure 3.** Morphological evolution of the solid during the reduction of hematite cubes at 800 °C, 60 % H<sub>2</sub> in He

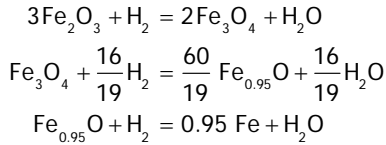
### Single pellet model

A mathematical model simulating the reduction of a single pellet was designed as a link between the experiments and the reactor model. Used independently, it helps to understand, analyze and simulate the reduction experiments. Used as a subroutine of the reactor model, it predicts the reaction rate as a function of the local reduction conditions (temperature and gas composition). This pellet model was built according to the experimental findings. The pellet (typically 12-mm diameter) is viewed as a cluster of grains (25 μm diameter), with an intergranular porosity of about 10 %. Grains are themselves porous (50% intra-grain porosity) and, in the case of wustite, assumed to be composed of dense crystallites (2 μm) separated by thin pores.

To keep the mathematical description simple, which is quite desirable for subsequent integration in REDUCTOR, we decided to use the concept known as the law of additive reaction times [8] for calculating the overall reaction rate. This law considers that mass transfer processes take place in series so that mass transfer resistances, represented by characteristic times, can be added. A single, complicated but analytical, relationship can be derived for the reaction rate. The law is approximate but its validity was demonstrated for several gas-solid systems [9]. Its top interest is its ability to represent intermediate (mixed) kinetic regimes in a closed-form equation, very fast to compute as a subroutine of larger reactor-scale codes.

The detailed equations used for calculating the different characteristic times and the corresponding reaction rates are given in [10]. The following phenomena are taken into account: mass transfer of H<sub>2</sub>

and H<sub>2</sub>O through the boundary layer surrounding the pellet, gas diffusion in the inter-grain pores, in the intra-grain pores, and in the pores of the iron layer around the crystallites, the last two ones involving Knudsen-type diffusion, solid phase diffusion of oxygen through the iron layer when it is dense, the three heterogeneous reactions of reduction,



and possible sintering of the iron phase.

The description of this last phenomenon is an original feature of our model, introduced to reflect two experimental observations: first, the reaction rate decrease noted (Figure 2, top) at high conversions and at temperatures greater than 850 °C; and second, the growth and densification of the iron grains (not shown) above the same temperature. We explain this behaviour by the tendency of the freshly formed iron layer, at the level of the crystallites, to sinter, i.e. to decrease its surface area. As a result, the intra-crystallite pores get thinner, which makes gas diffusion through these pores more difficult, and the pores eventually disappear, which makes solid diffusion, a slower process, the only possible mass transfer process for the rest of the reaction. The corresponding equations in the model are again given in [10].

Figure 4 gives the main results of the pellet model. The comparison with the experiment (top graph) shows that the model satisfactorily simulates the experiment. The slowing down at 80% conversion can be noted. The succession of the three reactions (hematite → magnetite → wustite → iron, bottom graph) is illustrated. Hematite disappears rapidly, whereas the reduction of wustite is the longest step.

### REDUCTOR: model of a shaft furnace operated with 100% H<sub>2</sub>

To predict the performance of the reactor, for a process that does not yet exist, mathematical modelling seemed to be the best suited approach. It can give access to all of the relevant variables of the process (local solid and gas temperatures, compositions and velocities, reactions rates, conversion, etc.). Our modelling approach is similar to CFD (computational fluid dynamics): it is based on the numerical solution of the local mass, energy and momentum balances. Therefore, beyond a global assessment of the process like obtained from flow-sheeting softwares, the detailed, spatially-resolved behaviour of the reactor can be known. Moreover, the influence of operating conditions and physical parameters can be analyzed quantitatively and optimal conditions derived.

REDUCTOR is a 2-dimensional (cylindrical coordinates), steady-state, numerical model. The principal

equations considered are the local mass, energy, and momentum balances written below. Notation:  $r$  = radius,  $z$  = height,  $c_i$  = total gas concentration,  $x_i$  = molar fraction of  $i$  in gas,  $u_g$  = superficial gas velocity,  $D_a$  and  $D_r$  = axial and radial dispersion coefficients,  $r_1$ ,  $r_2$ ,  $r_3$  = rates (mol s<sup>-1</sup> m<sup>-3</sup>) of the three reduction reactions: hematite → magnetite, magnetite → wustite and wustite → iron,  $w_j$  = mass fraction of  $j$  in solid,  $M_i$  = molar weight of  $i$ ,  $\rho_g$  = density of the gas,  $\rho_s$  = apparent density of the solid bed,  $c_{pg}$ ,  $c_{ps}$  = specific heat of the gas and solid,  $\lambda_g$  = thermal conductivity of the gas,  $T_g$ ,  $T_s$  = temperatures of the gas and solid,  $a_g$  = specific surface area of the bed,  $h$  = heat transfer coefficient,  $\lambda_{eff,a}$ ,  $\lambda_{eff,r}$  = axial and radial effective conductivities of the solid bed,  $\Delta_r H_i$  = heat of reaction  $i$ ,  $p$  = gas pressure,  $\varepsilon$  = inter-pellet porosity of the bed,  $d_p$  = diameter of the pellets,  $\mu_g$  = viscosity of the gas.

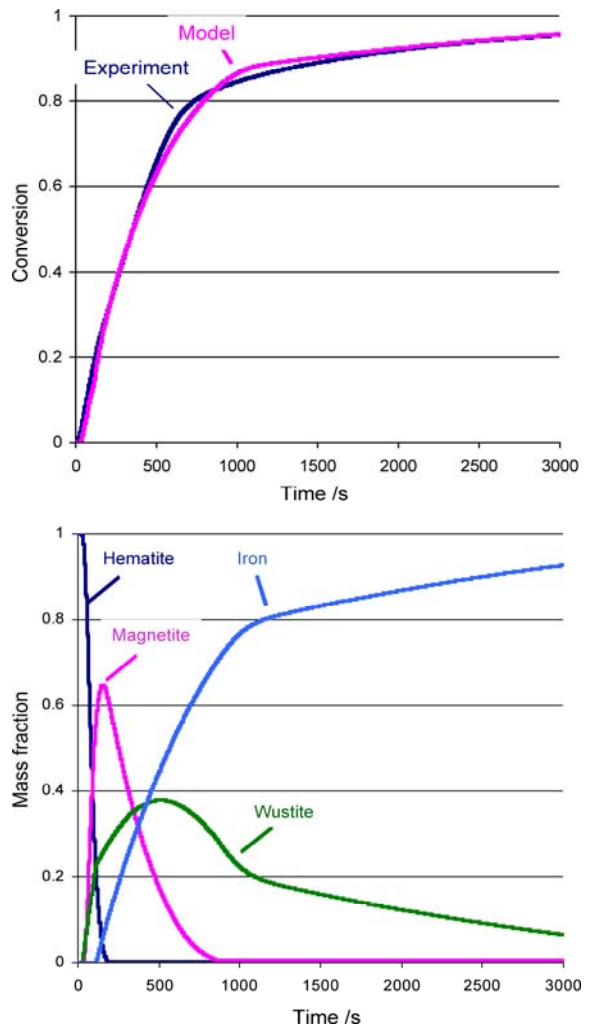


**Figure 4.** Results of the single pellet model, 900°C, 60 % H<sub>2</sub> in He. Top: comparison with experiment; bottom: evolution of the mass fractions of the different oxides and iron.

Mass balances for the gases:

$$\frac{1}{r} \frac{\partial (r c_i x_i u_{gr})}{\partial r} + \frac{\partial (c_i x_i u_{gz})}{\partial z} = \frac{1}{r} \frac{\partial}{\partial r} \left( r c_i D_r \frac{\partial x_i}{\partial r} \right) + \frac{\partial}{\partial z} \left( c_i D_a \frac{\partial x_i}{\partial z} \right) + S_i$$

with  $i = \text{H}_2$  or  $\text{H}_2\text{O}$  and  $-S_{\text{H}_2} = S_{\text{H}_2\text{O}} = r_1 + \frac{16}{19} r_2 + r_3$

Mass balances for the solids:

$$-\frac{\partial (\rho_s u_s w_j)}{\partial z} = S_j$$

with  $j = \text{Fe}_2\text{O}_3, \text{Fe}_3\text{O}_4, \text{Fe}_{0.95}\text{O}$ , or  $\text{Fe}$  and

$$S_{\text{Fe}_2\text{O}_3} = -3M_{\text{Fe}_2\text{O}_3} r_1$$

$$S_{\text{Fe}_3\text{O}_4} = M_{\text{Fe}_3\text{O}_4} (2r_1 - r_2)$$

$$S_{\text{Fe}_{0.95}\text{O}} = M_{\text{Fe}_{0.95}\text{O}} \left( \frac{60}{19} r_2 - r_3 \right)$$

$$S_{\text{Fe}} = 0.95 M_{\text{Fe}} r_3$$

Heat balance of the gas:

$$\rho_g c_{pg} \left( u_{gr} \frac{\partial T_g}{\partial r} + u_{gz} \frac{\partial T_g}{\partial z} \right) = \frac{1}{r} \frac{\partial}{\partial r} \left( r \lambda_g \frac{\partial T_g}{\partial r} \right) + \frac{\partial}{\partial z} \left( \lambda_g \frac{\partial T_g}{\partial z} \right) + a_g h (T_s - T_g) - \left( r_1 + \frac{16}{19} r_2 + r_3 \right) (c_{\text{PH}_2} - c_{\text{PH}_2\text{O}}) (T_g - T_s)$$

Heat balance of the solid:

$$-\rho_s u_s c_{ps} \frac{\partial T_s}{\partial z} = \frac{1}{r} \frac{\partial}{\partial r} \left( r \lambda_{\text{eff},r} \frac{\partial T_s}{\partial r} \right) + \frac{\partial}{\partial z} \left( \lambda_{\text{eff},a} \frac{\partial T_s}{\partial z} \right) + a_g h (T_g - T_s) + r_1 (-\Delta_r H_1) + r_2 (-\Delta_r H_2) + r_3 (-\Delta_r H_3) + \left( r_1 + \frac{16}{19} r_2 + r_3 \right) (c_{\text{PH}_2} - c_{\text{PH}_2\text{O}}) (T_g - T_s)$$

Momentum equation combined with gas continuity equation:

$$\frac{1}{r} \frac{\partial}{\partial r} \left( r \frac{c_t}{K} \frac{\partial p}{\partial r} \right) + \frac{\partial}{\partial z} \left( \frac{c_t}{K} \frac{\partial p}{\partial z} \right) = 0$$

with  $K = 150 \frac{(1-\varepsilon)^3}{\varepsilon^3 d_p^2} \mu_g + 1.75 \frac{(1-\varepsilon)}{\varepsilon^3 d_p} \rho_g u_g$

The reaction rates of the three reactions are those determined according to the single pellet model, which are derived from the kinetic experiments.

These partial derivative equations are complemented by the set of appropriate boundary conditions (known inlet temperatures and compositions, zero fluxes at the symmetry axis and wall, etc.). All details are given in [10], together with the correlations used for calculating the various physical, chemical, and thermal parameters.

The numerical solution is that of the finite volume method [11]: the partial derivative equations are rendered discrete and the resulting algebraic linear

system is iteratively solved using the Gauss-Seidel algorithm. Meshing involves 201 (vertical)  $\times$  21 (radial) cells. The code is written in Fortran 90. Computations were run using a PC cluster (16 processors AMD Opteron) and lasted typically 40 h.

A reference case was first simulated. The domain modelled corresponds only to the cylindrical section of the shaft furnace, where the reduction takes place, above the lateral reduction gas inlet. Figure 5 gives the geometry of the furnace modelled and the inlet flows. The solid flow rate corresponds to a production of  $1 \text{ Mt}_{\text{Fe}} \text{ yr}^{-1}$ , and the total gas flow rate ( $3734 \text{ mol s}^{-1}$ ) is 3.8 times the stoichiometric one.

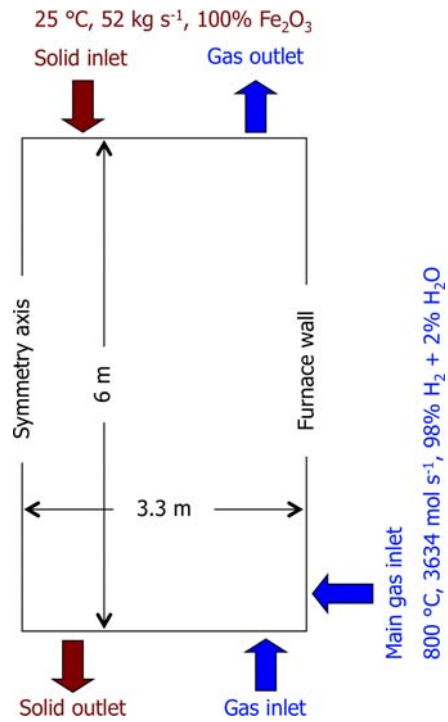
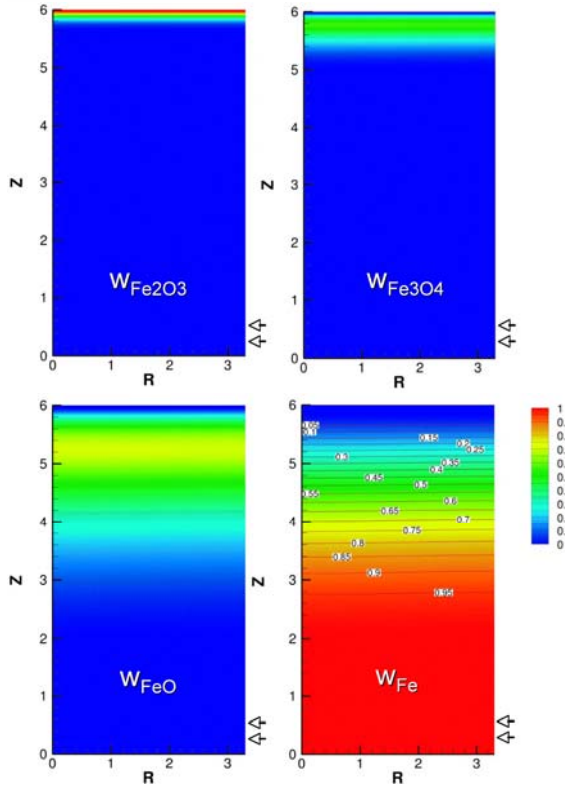


Figure 5. Conditions of computation in the reference case

Figure 6 shows the calculated mass fractions of the different oxides and iron.



**Figure 6.** Calculated mass fractions of the solid species in the reference case: gas in 800 °C, 98 %H<sub>2</sub>, d<sub>p</sub>=12 mm

Similar to the single pellet model, reductions of hematite and magnetite are fast. That of wustite takes longer but, at z=2 m, all oxides are fully converted to iron, irrespective of the radial position (in this simulation). This is an important result because it shows that about 4 m in height are required to obtain 100% Fe, whereas usual DR furnaces operated with syngas (CO+H<sub>2</sub>) are typically 9 m high (with the same 6.6-m diameter for a classical MIDREX furnace) and only permits one to attain 92 % Fe.

Other simulations were conducted to study the influence of operating conditions and physical parameters. For sake of brevity of the paper, only the effects of the water content of the inlet gas and of the pellet size will be reported here (Figure 7 and 8).

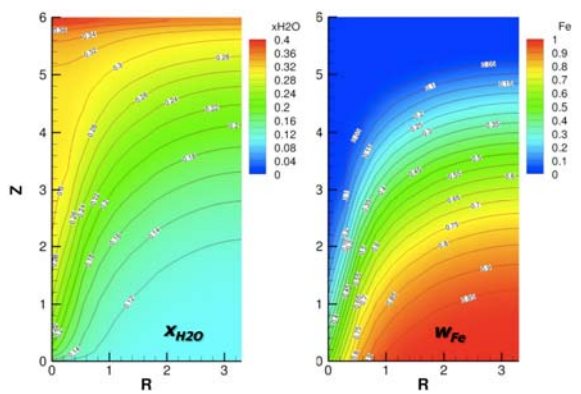


**Figure 7.** Calculated molar fractions of water vapour in the gas (left) and mass fraction of iron in the solid (right), when introducing 10% H<sub>2</sub>O in the gas

Introducing a higher water content in the gas decreases the driving force of the (reversible) reactions and thus the kinetics. The map of iron mass fractions with 10% water (Figure 7 right), when compared with that of the reference case where only 2% water were present in the injected reduction gas, shows that the reaction is not complete, in particular in the centre region.

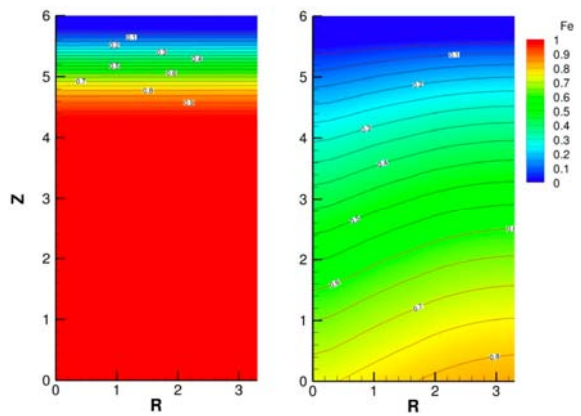


**Figure 8.** Calculated mass fractions of iron for different pellet sizes: d<sub>p</sub>=6 mm (left) and d<sub>p</sub> =24 mm (right)

When changing the pellet size, with 24-mm diameter pellets, the conversion is not complete (75 % Fe on average at outlet), whereas with 6-mm pellets, a full conversion is obtained only 2 m downstream from the solid inlet, which can be compared to 4 m with the 12-mm pellets of the reference case. Therefore, decreasing the pellet size seems a quite attractive option for the industrial practice.

### Conclusion

REDUCTOR, a new, steady-state, 2-dimensional, CFD-type model of a shaft furnace operated with pure hydrogen has been developed. It describes gas and solid flows, mass and heat transfers, and the three-reaction reduction of hematite to iron. Kinetics are expressed using a specific single pellet model based on the law of additive reaction times and experimental data. First results confirm the high potential of hydrogen direct reduction: CO<sub>2</sub> emission of the reactor itself is zero and, due to the faster kinetics of iron oxides reduction with hydrogen (compared with CO), a full conversion to iron can be obtained with a much smaller reactor (typically half the size) than usual MIDREX or HYL direct reduction furnaces. Future work on this model will consist in taking into account CO, and the related chemical reactions, to be able to simulate current DR processes and thus to validate the model against plant data.

## Acknowledgements

The authors thank all the ULCOS SP4 and SP12 partners for interesting exchanges on this piece of work, and Dr. J.P. Birat, ULCOS chairman, for his continuous support.

The present work is part of the ULCOS program, which operates with direct financing from its 48 partners, especially of its core members (Arcelor-Mittal, Corus, TKS, Riva, Voestalpine, LKAB, Saarstahl, Dillinger Hütte, SSAB, Ruukki and Statoil), and has received grants from the European Commission under the 6<sup>th</sup> Framework RTD program and the RFCS program<sup>1</sup>.

## References

- [1] <http://www.ulcos.org>.
- [2] H.Y. Sohn, "Suspension Hydrogen Reduction of Iron Oxide Concentrate", 2008, US DoE report, DE-FC36-97ID13554, <http://www.osti.gov/bridge/purl.cover.jsp?purl=/929441-7IDUA4/>.
- [3] ULCOS SP4 conclusions, ULCOS internal report, 2006.
- [4] E. T. Turkdogan and J. V. Vinters, "Gaseous Reduction of Iron Oxides.1. Reduction of Hematite in Hydrogen", Metallurgical Transactions, 2 (11) (1971), 3175-3188.
- [5] D. H. St John and P. C. Hayes, "Microstructural Features Produced by the Reduction of Wustite in H<sub>2</sub>/H<sub>2</sub>O Gas-Mixtures", Metallurgical Transactions B-Process Metallurgy, 13 (1) (1982), 117-124.
- [6] M. Moukassi, P. Steinmetz, B. Dupre and C. Gleitzer, "Mechanism of reduction with hydrogen of pure wustite single crystals", Metallurgical Transactions B: Process Metallurgy, 14B (1) (1983), 125-32.
- [7] Towhidi, N. and J. Szekely, "The influence of carbon deposition on the reduction kinetics of commercial grade hematite pellets with CO, H<sub>2</sub>, and N<sub>2</sub>" Metallurgical Transactions B (14) (1983), 3, 359-367.
- [8] Sohn, H. Y., "The law of additive reaction times in fluid-solid reactions" Metallurgical Transactions (9B) (1978), 89-96.
- [9] F. Patisson, B. Dussoubs, and D. Ablitzer "Using Sohn's law of additive reaction times for modeling a multiparticle reactor. The case of the moving bed furnace converting uranium trioxide into tetrafluoride", Sohn International Symposium "Advanced processing of metals and materials", 27-31 Aug. 06, San Diego. Proceedings edited by F. Kongoli and R.G. Reddy, TMS, vol. 1 "Thermo and physicochemical principles: non-ferrous high-temperature processing", pp. 141-153. <http://hal.archives-ouvertes.fr/hal-00265646/fr/>.
- [10] D. Wagner, "Etude expérimentale et modélisation de la réduction du minerai de fer par l'hydrogène", PhD dissertation, 2008, Nancy-Université, <http://tel.archives-ouvertes.fr/tel-00280689/fr/>.
- [11] Patankar, S. V. (1980), "Numerical heat transfer and fluid flow". New York, Hemisphere Publishing Corp.

---

<sup>1</sup> Priority 3 of the 6<sup>th</sup> Framework Programme in the area of "Very low CO<sub>2</sub> Steel Processes", in co-ordination with the 2003 and 2004 calls of the Research Fund for Coal and Steel